# Self-assembly of Dumbbell-shaped Rod Amphiphiles Based on Dodeca-*p*-phenylene

**Zhegang Huang, Libin Liu, Eunji Lee, and Myongsoo Lee***

*Center for Supramolecular Nano-Assembly and Department of Chemistry, Yonsei University, Seoul 120-749, Korea*
**E-mail: mslee@yonsei.ac.kr*
*Received March 11, 2008*

Dumbbell-shaped aromatic amphiphilic molecules consisting of a dodeca-*p*-phenylene as a rigid segment and oligoether dendrons as a flexible chains were synthesized, characterized, and their aggregation behavior was investigated in the bulk and at the air-water interface. In contrast to the molecule **2** which shows a nematic liquid crystalline state, molecule **1** based on shorter dendritic chains was observed to self-assemble into a 3-D primitive orthorhombic supercrystal. And molecule **1** at the air-water interface was observed to reorganize from circular plates to ring structures by lateral compressions.

**Key Words :** Dumbbell-shape, Self-assembly, Nanocrystal, Nanoring, Circular plate

## Introduction

The creation of supramolecular units through self-assembly process is one of the most exciting research in interdisciplinary areas combining chemistry, biology and material science.[1-3] Among self-assembling molecular systems, rod-coil block molecules provide a facile entry to used for construction of supramolecular architectures with well defined shape.[4] The supramolecular structures can be precisely controlled by systematic variation of the type and relative length of the respective block in various solution, bulk, surface, and interfacial environments.[5-7] Incorporation of a flexible hydrophilic dendritic branches into the conjugated rod building block leads to a tree-shaped molecules has been reported to have a large impact to self-organize into unique aggregation structures, such as discrete bundles, ribbons, and vesicles.[8]

One can envision that incorporation of a conjugated rod into an amphiphilic dumbbell-shaped molecular architecture, by grafting a flexible dendrons to its both ends of a rod would frustrate a parallel arrangement of the rod segments commonly observed for linear rod-coil molecules, in order to minimize a steric repulsion between bulky segments.[9] In addition, previous experiments from our laboratory have demonstrated that the amphiphilic dumbbell-shaped molecule gives rise to the formation of a helical nanofibers, consisting of hydrophobic aromatic cores surrounded by hydrophilic flexible segments that are exposed to the aqueous environment.[10] These results imply that the molecular dumbbell extends the supramolecular organization capabilities of conjugated aromatic rods. As an extension of this study to further investigate their ability to assemble into organized structures in the bulk and at the air-water interface, we have synthesized amphiphilic dumbbell-shaped molecules **1**.

## Experimental Section

**Measurements.** $^1$H-NMR spectra were recorded from $CDCl_3$ or DMSO solutions on a Bruker AM 250 spectrometer. A Nikon Optiphot 2-pol optical polarized microscopy (magnification: 300 ×) equipped with a Mettler FP 82 hot-stage and a melttler FP 90 central processor was used to observe the thermal transitions and to analyze the anisotropic texture. A Perkin Elmer DSC-7 differential scanning calorimeter equipped with 1020 thermal analysis controller was used to determine the thermal transitions, which were reported as the maxima and minima of their endothermic or exothermic peaks. In all cases, the heating and cooling rates were 10 °Cmin$^{-1}$. X-ray scattering measurements were performed in transmission mode with synchrotron radiation at the 10C1 X-ray beam line at Pohang Accelerator Laboratory, Korea. MALDI-TOF-MS was performed on a perseptive

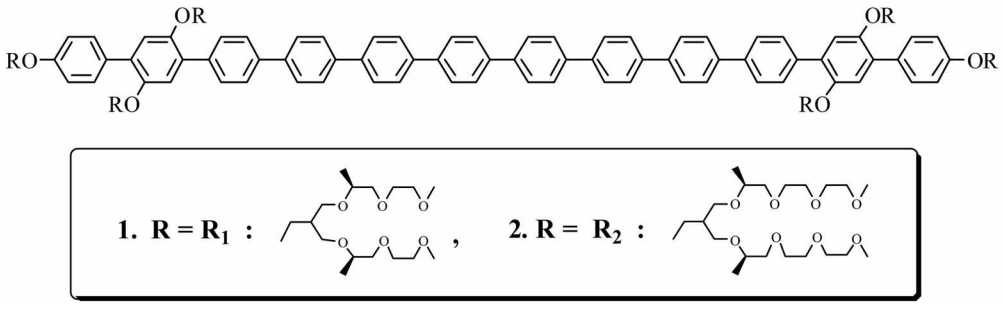


**Chart 1**. Molecular structures of 1 and **2**.

Biosystems Voyager-DE STR using a 2,5-dihydroxy benzoic acid matrix. Preparative high performance liquid chromatography (HPLC) was performed at room temperature using a 20 mm × 600 mm poly styrene column on a Japan Analytical Industry Model LC-908 recycling preparative HPLC system, equipped with UV detector 310 and RI detector RI-5. The transmission electron microscope (TEM) was performed at 120 kV using JEOL 2010. The molecular films were fabricated using usual Langmuir technique on a KSV minitrough system (KSV Instrument Ltd).[11] The transferred films were scanned in tapping mode under ambient conditions with a Veeco NanoScope IIIa AFM (Digital Instruments, Inc., Santa Barbara, CA ) using Nanosensors silicon probes (dimensions: T = 3.5-4.5 $\mu$m, W = 30-40 $\mu$m, L = 115-135 $\mu$m).

**Synthesis.** Chlorotrimethylsilane (98%), tetrakis(triphenylphosphine)palladium(0) (99%), *n*-butyllithium (1.6 M solution in *n*-hexane), 4,4'-dibromobiphenyl (98%), borane-THF complex (1.0 M solution in THF), borontribromide (1.0 M solution in dichloromethane), *p*-toluenesulfonylchloride (98 %), triisopropylborate (98%), bisbenzonitrilepalladium(II) dichloride, tetradimethylaminoethylene (TDAE) (98%), iodinemonochloride (1.0 M solutuion in dichloromethane), 4-bromoanisole (99%), (all from Aldrich) and the conventional reagents were used as received. Flash chromatography was carried out with Silica Gel 60 (230-400 mesh) from EM Science. Dried THF was obtained by vacuum transfer from sodium and benzophenone. The compounds **3a**, **2**, and ether-type dibranched coils ($R_1$) were prepared according to similar procedures described previously.[8a,10,12] The general synthetic routes for 1 are shown in Scheme 1.

**Synthesis of compound 3b.** Compound **3a** (0.17 g, 0.36 mmol), $R_1OTs$ (0.59 g, 1.2 mmol) and $K_2CO_3$ (0.33 g, 2.4 mmol) were dissolved in $CH_3CN$ (30 mL). The reaction mixture was refluxed for 72 h under nitrogen. Cooled to room temperature, water (100 mL) was added and the aqueous layer was washed twice with ethyl acetate. The combined organic layer was dried over anhydrous $MgSO_4$ and filtered. The solvent was removed in a rotary evaporator. The crude product was purified by column chromatography (silica gel, ethyl acetate followed by THF to yield 0.31 g (63%) of a colorless oil; $^1$H-NMR (250 MHz, $CDCl_3$) 1.04-1.16 (m, 18H, 6 × CH$CH_3$), 2.2-2.5 (m, 3H, 3 × $CH$($CH_2$)$_3$), 3.31 (s, 18H, 6 × O$CH_3$), 3.32-3.61 (m, 54H, $OCH_2$), 3.99-4.11 (m, 6H, 3 × $CH_2$OPh), 6.92-7.00 (m, 4H, o to $OCH_2$), 7.38 (d, 2H, m to I, $J$ = 8.4 Hz), 7.49 (d, 2H, m to $OCH_2$, $J$ = 8.6 Hz), 7.57-7.63 (m, 4Ar-H), 7.78 (d, 2H o to I, $J$ = 8.4 Hz).

**Synthesis of compound 4a.** Compound **3b** (0.31 g, 0.22 mmol) and 4-trimethyl silyl-biphenyl-4'-boronic acid (72.7 mg, 0.27 mmol) were dissolved in degassed THF (25 mL). Degassed 2 M aqueous $Na_2CO_3$ (25 mL) was added to the solution and then tetrakis(triphenylphosphine)palladium(0) (2.9 mg, 2.5 $\mu$mol) was added. The mixture was refluxed for 24 h with vigorous stirring under nitrogen. Cooled to room temperature, the layers were separated, the aqueous layer was washed twice with ethyl acetate. The combined organic layer was dried over anhydrous $MgSO_4$ and filtered. The solvent was removed in a rotary evaporator, and the crude products was purified by column chromatography (silica gel, ethyl acetate followed by THF) to yield 0.32 g (97%) of a light yellow oil: $^1$H-NMR (250 MHz, $CDCl_3$, $\delta$, ppm) 0.32 (s, 9H, $(CH_3)_3$Si), 1.06-1.17 (m, 18H, 6 × CH$CH_3$), 2.2-2.5 (m, 3H, 3 × $CH$($CH_2$)$_3$), 3.32 (s, 18H, 6 × O$CH_3$), 3.33-3.72 (m, 54H, $OCH_2$), 3.61-4.11 (m, 6H, 3 × $CH_2$OPh), 6.92-7.00 (m, 4H, o to $OCH_2$), 7.50 (d, 2H, m to $OCH_2$, $J$ = 8.6 Hz), 7.62-7.76 (m, 16Ar-H).

**Synthesis of compound 4b.** To a solution of compound **4a** (0.33 g, 0.22 mmol) in $CH_2Cl_2$ at −78 °C was dropped 1.0 M solution of ICl in $CH_2Cl_2$ (0.45 mL). The reaction mixture was stirred over 2 h under nitrogen. 1 M aqueous $Na_2S_2O_5$ solution was added and stirred over 1 h. The layers were separated, the aqueous layer was washed twice with $CH_2Cl_2$. The combined organic layer was dried over anhydrous $MgSO_4$ and filtered. The solvent was removed in a rotary evaporator, and the crude products was purified by column chromatography (silica gel, ethyl acetate followed by THF) to yield 0.27 g (79%) of a light yellow oil; $^1$H-NMR (250 MHz, $CDCl_3$, $\delta$, ppm) 1.05-1.17 (m, 18H, 6 × CH$CH_3$), 2.2-2.5 (m, 3H, 3 × $CH$($CH_2$)$_3$), 3.32 (s, 18H, 6 × O$CH_3$), 3.33-3.72 (m, 54H, $OCH_2$), 3.61-4.11 (m, 6H, 3 × $CH_2$OPh), 6.93-7.04 (m, 4Ar-H, o to $OCH_2$), 7.38 (d, 2H, m to I, $J$ = 8.4 Hz), 7.49 (d, 2H, m to $OCH_2$, $J$ = 8.6 Hz), 7.67-7.79 (m, 14Ar-H).

**Synthesis of compound 1.** Compound **4b** (0.27 g, 0.17 mmol), and TDAE (0.023 g 0.34 mmol) were dissolved in DMF (30 mL). And then $Pd(PhCN)_2Cl_2$ (0.002 g, 0.005 mmol) was added. The mixture was heated at 50 °C for 4 h with stirring under nitrogen. Cooled to room temperature, the DMF solvent were removed under vacuum distillation, and the crude products was purified by column chromatography (silica gel, ethyl acetate followed by THF) and precipitated by $CH_2Cl_2$ and *n*-hexane to yield 0.186 g (75%) of a yellow liquid: $^1$H-NMR (250 MHz, $CDCl_3$, $\delta$, ppm) 1.01-1.16 (m, 36H, 12 × CH$CH_3$), 2.2-2.5 (m, 6H, 6 × $CH$($CH_2$)$_3$), 3.32 (s, 36H, 12 × O$CH_3$), 3.33-3.72 (m, 108H, $OCH_2$), 3.61-4.11 (m, 12H, 6 × $CH_2$OPh), 6.82-6.96 (m, 8Ar-H, o to $OCH_2$), 7.46(d, 4Ar-H, m to $OCH_2$, $J$ = 8.6 Hz), 7.64-7.79 (m, 32Ar-H) $^{13}$C-NMR (100 MHz, $CDCl_3$, ppm): $\delta$ = 158.75, 150.40, 139.90, 138.76, 137.57, 130.81, 130.34, 129.53, 127.71, 126.66, 115.26, 114.19, 75.45, 75.33, 75.24, 75.10, 72.26, 72.21, 70.98, 70.93, 67.45, 59.33, 59.28, 40.85, 17.41, 17.30. Anal. Calcd for $C_{168}H_{242}O_{42}$: C, 68.78; H, 8.31; Found C, 68.83 ; H, 8.29. MALDI-TOF-MS m/z $(M+H)^+$ 2933.06, $(M+Na)^+$ 2956.18.

## Results and Discussion

The synthesis of dumbbell-shaped molecule **2** has been reported and its analogous **1** with the short dendritic chains has been synthesized in a similar stepwise fashion as outlined in Scheme 1. The starting materials, dibranched coil and molecule **3a** were preprared according to the procedures described previously.[8a,12] The flexible coil-substituted tetraphenyl derivative **3b** was prepared by etherification with

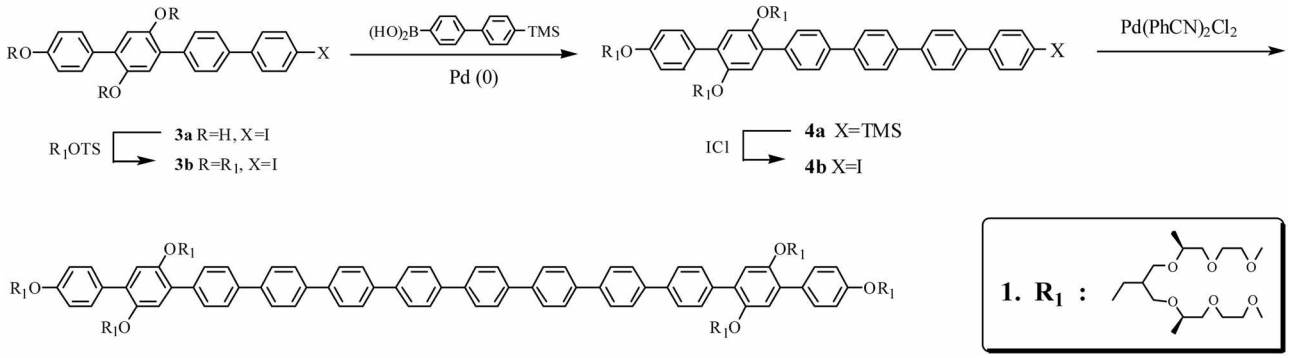


**Scheme 1**. Synthesis of molecules 1.

tosylated oligoether dendrons. The resulting compound was elongated by Suzuki coupling with 4-trimethylsilyl-4'-biphenylboronic acid and yielded compound **4a**. For the next Suzuki coupling reaction, the silyl group of **4a** was substituted to aryl iodine, which is the most active in Suzuki-type aromatic couplings, and then the final molecule was synthesized by palladium-catalyzed homocoupling reaction of the precursor molecules.

The resulting molecule **1** was characterized by $^{1}H$ and $^{13}C$ NMR spectroscopy, elemental analysis and matrix-assisted laser desorption ionization time-of-flight (MALDI-TOF) mass spectroscopy and were shown to be in full agreement with the structures presented. As confirmed by $^{1}H$ NMR spectroscopy, the ratio of the aromatic protons of the rod block to the alkyl protons is consistent with the ratio calculated, and the MALDI-TOF mass spectra of the molecules exhibit two signals that can be assigned as the $H^+$ and $Na^+$ labeled molecular ions. The mass corresponding to a representative peak in the spectrum is matched with the calculated molecular weight of each molecule.

**Solid state structure.** The self-assembling behavior of the dumbbell-shaped molecules in the bulk was investigated by means of DSC, thermal optical polarized microscopy, TEM and X-ray scatterings. The molecules show an ordered structure, and the transition temperatures and the corresponding enthalpy changes are determined from DSC scans (Figure 1a). As can be observed from Figure 1a, molecule **1** melts into a birefringent liquid crystalline phase at 68 °C, followed by isotropic liquid at 188 °C. On slow cooling from the isotropic liquid of **1**, a schlieren texture above 180 °C appeared and then a rectangular areas growing in four directions can be observed with a final development of mosaic texture, corresponding to a nematic and a tetragonal phase respectively (Figure 1b).[13]

To identify the tetragonal phase structure of molecule **1**, small- and wide-angle X-ray scattering experiments were performed. The small-angle X-ray diffraction pattern of **1** shows three strong reflections together with a number of low intensity reflections at higher angles (Figure 2a), indicative of the existence of a highly ordered nanoscopic structure with three distinct lattice parameters. These reflections indeed can be indexed as a 3-D primitive orthorhombic structure with lattice parameters a = 8.3 nm, b = 5.6 nm, and

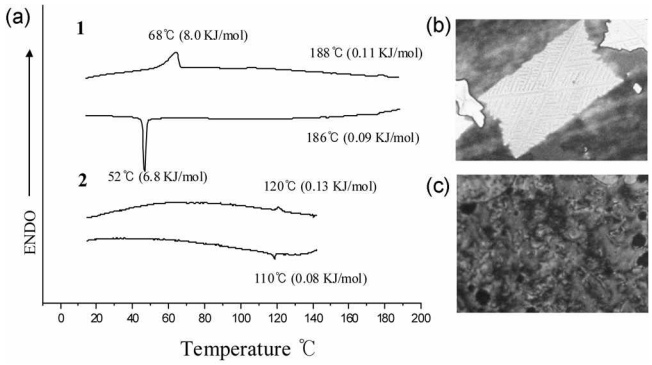


**Figure 1**. (a) DSC curves of dumbbell-shape molecules **1** and **2**. (b) Representative optical polarized micrograph (100 ×) of the texture exhibited by a primitive orthorhombic structure for **1**. (c) Representative optical polarized micrograph (100 ×) of the texture exhibited by nematic structure for **2** at the transition from the isotropic liquid state.

c = 3.4 nm. The wide-angle X-ray diffraction pattern shows several sharp reflections corresponding to a rectangular lattice with unit cell dimensions of x = 5.8 Å and y = 9.0 Å, indicating that the rod building blocks are arranged in a herringbone fashion within a domain (Figure 2b). To better understand the packing arrangement, we calculated the number (n) of molecules in each bundle. Calculated from the lattice constants determined from X-ray patterns and measured densities, the average number (n) of molecules in a unit cell was estimated to be approximately 37.

To further confirm the formation of a 3-D structure, molecule **1** was cryomicrotomed to a thickness of *ca.* 50-70 nm and then stained with $RuO_4$ vapor, and observed by transmission electron microscopy (TEM). As shown in Figure 3, the dark rod domains are regularly arrayed in a light flexible chain matrix and the interdomain distances were measured to be approximately 8 nm and 5 nm, which are consistent with those obtained from X-ray scattering (Figure 3).

On the basis of the optical and transmission electron microscopic observations and X-ray diffraction results, dumbbell-shaped molecule **1** could be considered to self-assemble into descrete bundles surrounded by flexible ether chains that organize into a 3-D primitive orthorhombic supercrystal (Figure 4).

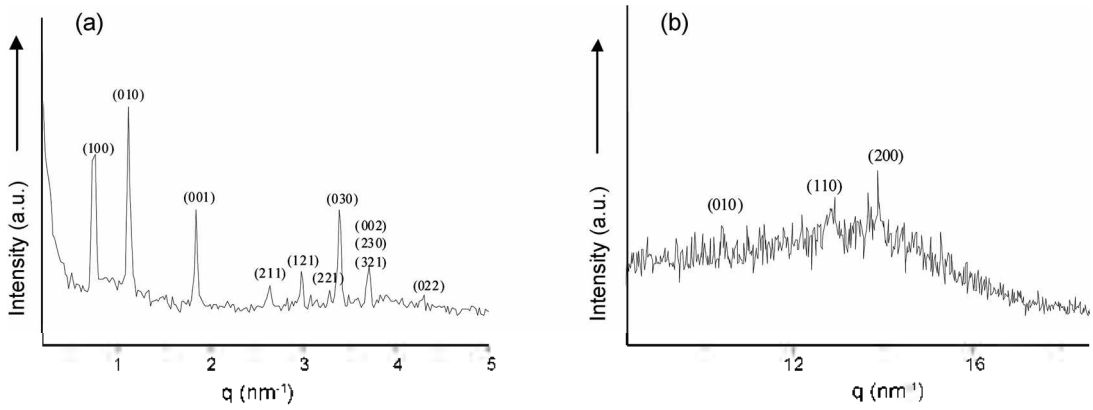


**Figure 2**. (a) Small-angle X-ray diffraction pattern of 1 measured at 55 °C, (b) wide-angle X-ray diffraction pattern of 1 measured at 55 °C.

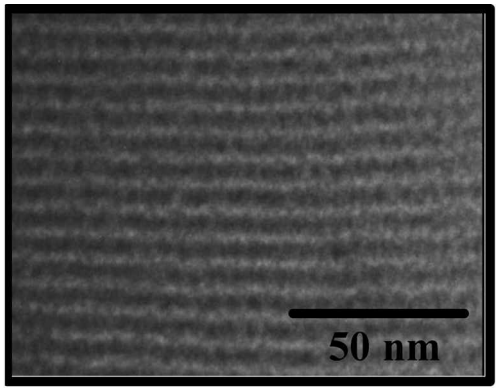


**Figure 3**. TEM images of ultramicrotomed films of 1 stained with $RuO_4$ revealing an ordered array of alternating light colored dendritic layers and dark aromatic layers.

In contrast, molecule **2** based on an elongated coil block shows a liquid crystalline phase that transform into isotropic liquid at 120 °C. In POM analysis, a schlieren like texture appeared from the isotropic liquid above 115 °C, corresponding to a nematic liquid crystalline structure (Figure 1c). The lack of crystallinity in the rod building blocks of this molecule is most likely due to confinement between larger cross-sectional area. Both steric forces and crystallization are believed to play an important role in the formation of discrete bundle. Dumbbell-shaped molecules based on a small flexible coil would be packed into a discrete 3-D solid structure as in the case of **1**. Increasing the volume fraction of the coil causes the steric forces among the interface parts to be greater.[14] This increase in steric repulsion could frustrate 3-D ordering of the rod building blocks to transform into a nematic liquid crystalline structure that allows more space for the flexible chains to adopt a less strained conformation. Accordingly, **2** based on longer flexible chains is likely to self-organize into a nematic structure.

**Surface microstructure.** Dumbbell-shaped molecule **1** displayed an amphiphilic behavior at the air-water interface and typical $\pi$-A curve is represented in Figure 5. A plateau was observed at the molecular area of 3.78 $nm^2$ and the followed surface pressure increased to 40 mN/m, indicating the monolayer completely collapsed. The limiting cross-sectional surface area/molecule ($A_0$) calculated by the extrapolation of the steep rise in the surface pressure to a zero level is 3.36 $nm^2$ similar to calculated theoretical surface area of 3.28 $nm^2$ occupied by the hydrophobic rod block.

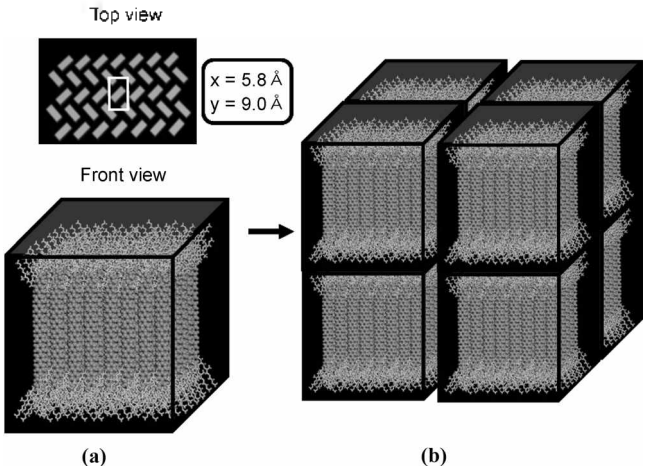


**Figure 4**. Schematic representation of (a) the self-assembly of 1 into a discrete bundle with the herringbone packing and (b) the subsequent crystallization into a primitive orthorhombic superlattice.

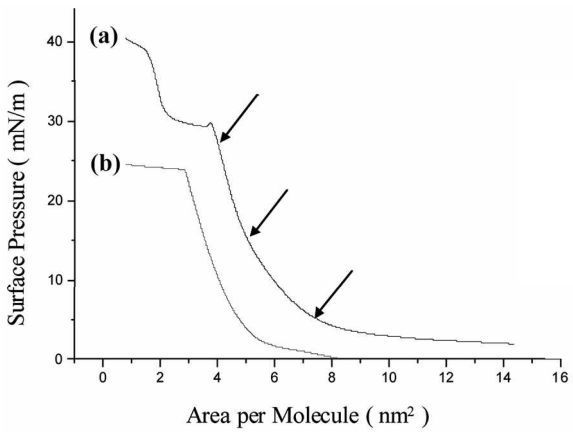


**Figure 5**. Surface pressure-area isotherms of dumbbell-shaped molecules. (a) $\pi$-A isotherms of molecule 1 and (b) $\pi$-A isotherms of molecule **2** with deposition points indicated by arrows.

indicating the aromatic rod segments adopt a face-on orientation rather than a titled orientation at the air-water interface. The complete pressure-area isotherm for the molecule **2** with longer dendritic groups was technically difficult to obtain due to the tendency of the molecules sink into the subphase at higher lateral compression.[15] The transferred films revealed only uniform surface topography without any signs of characteristic surface micellar structures.

To identify the surface morphologies of molecule **1**, atomic force microscopy (AFM) experiments were performed (Figure 6). At low surface pressure of 5 mN/m, circular plates were observed with a diameter of $30 \pm 4$ nm, accounting for the lateral broadening tip effect.[15] where the ethylene oxide chains spread on the water surface to form shell and the rods form core due to the $\pi$-$\pi$ interaction (Figure 6a). Considering the molecular length of 7.8 nm, we suggest that the circular plate should be composed of 5-7 molecules (Figure 6d). Upon compression to a modest surface pressure of 15 mN/m (onset of solid monolayer), the circular plates were compressed more densely and finally reorganized into ring-shaped domains caused by desorption of the ethylene oxide groups from the air-water interface into aqueous phase and the $\pi$-$\pi$ interaction of rod segments (Figure 6b). These ring structures were analyzed by multiple cross-sections and found to have an average external diameter of 17-22 nm with an interior diameter smaller than 10 nm according to the packing density (Figure 6e). Further compression leads to the monolayer collapse and high domains formation as revealed by AFM (Figure 6c). Besides the presence of the rings, the spheres with prolonged tails were irregularly arranged on the silicon substrate.

The reorganization of circular plates to ring structure by lateral compressions could be related to the folding of the flexible dendron and their dehydration due to expelling associated water molecules from densely packed area to the air-water interface beneath.[17] Due to the large cross-sectional mismatch between the hydrophobic rods and hydrophilic branches, spherical or cylindrical aggregates should be preferably formed in the solution as was already reported.[18] The two-dimensional limits of these highly curved spherical aggregates are circular structures which can fill out on a planar interface. Upon compression, the circular structures were more densely and further fused into ring structures. At condensed state, to relieve the steric repulsions without sacrificing $\pi$-$\pi$ stacking interactions between the rods, the hydrophilic dendron chains would sink into the aqueous phase that allow more space for the rigid rod to adopt a less strained conformation. The spectroscopic measurements further support the reorganization of circular pltes to ring structure. Figure 7 shows the absorption and fluorescence spectra of molecule 1 at continued compression from 5 to 15 mN $m^{-1}$ and of the $CHCl_3$ solution of **1** for comparison. Both the absorption and emission spectra of LB films appear to be red-shifted with respect to those of the corresponding solutions, demonstrating the aggregation of conjugated rod core segments.[19] At the initial compression up to 5 mN $m^{-1}$, the absorption spectrum exhibits a broad transition with a maximum at 358 nm. However, the absorption maximum is blue shifted with continued compression from 5 to 15 mN $m^{-1}$. Concurrently, the fluorescence is dramatically quenched at the transition from high surface pressure to low surface

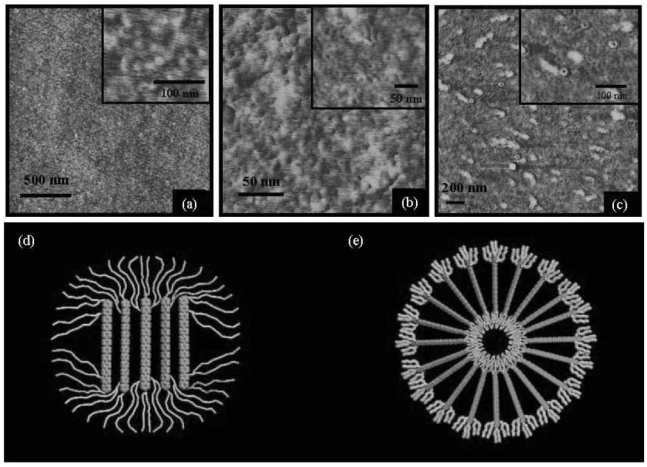


**Figure 6**. AFM topographical images of LB monolayer from molecule 1 (a) at surface pressure of 5 mN/m, (b) at surface pressure of 15 mN/m, (c) at surface pressure of 25 mN/m and schematic representation of **1** (d) self-organize into circular plate structure and (e) ring structure.

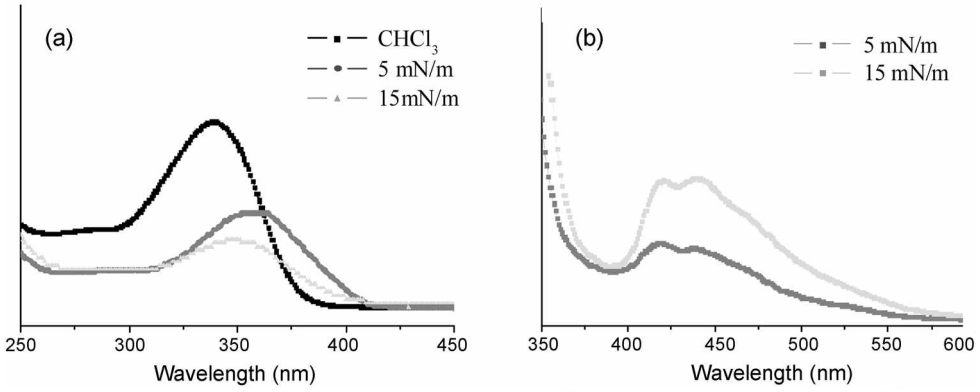


**Figure 7**. (a) Uv-vis absorption spectra of molecule 1 in chloroform, at surface pressure of 5 mN/m and at surface pressure 15 mN/m. (b) Fluorescence emission of molecule 1 at surface pressure of 5 mN/m and at surface pressure 15 mN/m.

pressure. This trend could be attributed to the extent of $\pi$-stacking overlap between adjacent rods, which is consistent with a proposed structural variation.[20,21]

## Conclusion

Dumbbell-shaped amphiphilic molecules consisting of dodeca-*p*-phenylene as a stem and oligo(ethylene oxide) dendrons as a branch were synthesized, characterized, and their self-assembling behavior was investigated in the solid and at the air-water interface. In contrast to **2**, which shows only nematic liquid crystalline state, molecule **1** self-assembles into discrete nanostructures that self-organized into a 3-D primitive orthorhombic supercrystal. At the air-water interface, molecular dumbbell **1** was reorganized from circular plate to ring structure by lateral compressions. These results demonstrate that rational design of a dumbbell-shaped amphiphilic molecule based on a conjugated rod building block allows discrete nanostructures by frustration of the parallel packing of the rod segments in the bulk and at the air-water interface.

**Acknowledgements.** This work was supported by the Creative Research Initiative Program of the Ministry of Science and Technology, Korea. We acknowledge a fellowship of the BK21 program from the Ministry of Education and Human Resources Development.

## References

1. (a) Cormelissen, J. J. L. M.; Rowan, A. E.; Nolte, R. J. M.; Sommerdijk, N. A. J. M. *Chem. Rev.* **2001**, *101*, 4039. (b) Hoeben, F. J. M.; Jonkheijm, P.; Meijer, E. W.; Schenning, A. P. H. H. *Chem. Rev.* **2005**, *105*, 1491.
2. (a) Motoyanagi, J.; Fukushima, T.; Ishii, N.; Aida, T. *J. Am. Chem. Soc.* **2006**, *128*, 4220. (b) Ajayaghosh, A.; Vijayakumar, C.; Varghese, R.; George, S. J. *Angew. Chem. Int. Ed.* **2006**, *45*, 456. (c) Chen, B.; Baumeister, U.; Pelzl, G.; Das, M. K.; Zeng, X.; Ungar, G.; Tschierske, C. *J. Am. Chem. Soc.* **2005**, *127*, 16578. (d) Percec, V.; Dulcey, A.; Balagurusamy, V. S. K.; Miura, Y.; Smidrkal, J.; Peterca, M.; Nummelin, S.; Edlund, U.; Hudson, S. D.; Heiney, P. A.; Duan, H.; Magonov, S. N.; Vinogradov, S. A. *Nature* **2004**, *430*, 764.
3. (a) Kawano, S.-I.; Fujita, N.; Shinkai, S. *J. Am. Chem. Soc.* **2004**, *126*, 8592. (b) Kuroiwa, K.; Shibata, T.; Takada, A.; Nemoto, N.; Kimizuka, N. *J. Am. Chem. Soc.* **2004**, *126*, 2016. (c) Antonietti, M.; Förster, S. *Adv. Mater.* **2003**, *15*, 1323.
4. (a) Lee, M.; Cho, B.-K.; Zin, W.-C. *Chem. Rev.* **2001**, *101*, 3869. (b) Yoo, Y.-S.; Lee, M. *J. Mater. Chem.* **2005**, *15*, 419. (c) Ryu, J.-H.; Cho, B.-K.; Lee, M. *Bull. Korean Chem. Soc.* **2006**, *27*, 1270.
5. Park, S.; Lim, J.-H.; Chung, S.-W.; Mirkin, C. A. *Science* **2004**, *303*, 348.
6. Stupp, S. I.; LeBonheur, V.; Walker, K.; Li, L. S.; Huggins, K. E.; Keser, M.; Amstutz, A. *Science* **1997**, *276*, 384.
7. (a) Schenning, A. P. H. J.; Elissen-Roman, C.; Weener, J.; Baars, M. W. P. L.; Van der Gaast, S. J.; Meijer, E. W. *J. Am. Chem. Soc.* **1998**, *120*, 8199. (b) Tsukruk, V. V. *Adv. Mater.* **1998**, *10*, 253.
8. (a) Yoo, Y.-S.; Choi, J.-H.; Song, J.-H.; Oh, N.-K.; Zin, W.-C.; Park, S.; Chang, T.; Lee, M. *J. Am. Chem. Soc.* **2004**, *126*, 6294. (b) Holzmueller, J.; Genson, K. L.; Park, Y.; Yoo, Y.-S.; Park, M.-H.; Lee, M.; Tsukruk, V. V. *Langmuir* **2005**, *21*, 6392.
9. (a) Mori, A.; Yokoo, M.; Hashimoto, M.; Ujiie, S.; Diele, S.; Baumeister, U.; Tschierske, C. *J. Am. Chem. Soc.* **2003**, *125*, 6620. (b) Xu, Y.; Leng, S.; Xue, C.; Sun, R.; Pan, J.; Ford, J. Jin, S. *Angew. Chem. Int. Ed.* **2007**, *46*, 3896. (c) Huang, Z.; Ryu, J.; Lee, E.; Lee, M. *Chem. Mater.* **2007**, *19*, 6569.
10. Bae, J.; Choi, J.-H.; Yoo, Y.-S.; Oh, N.-K.; Kim, B.-S.; Lee, M. *J. Am. Chem. Soc.* **2005**, *127*, 9668.
11. Ulman, A. *An Introduction to Ultrathin Organic Films*; Academic Press: San Diego, CA, 1991.
12. Kim, H.-J.; Zim, W.-C.; Lee, M. *J. Am. Chem. Soc.* **2004**, *126*, 7009.
13. Lee, M.; Cho, B.-K.; Jang, Y.-G.; Zin, W.-C. *J. Am. Chem. Soc.* **2000**, *122*, 7449.
14. Lee, M.; Jeong, Y.-S.; Cho, B.-K.; Oh, N.-K.; Zin, W.-C. *Chem.-Eur. J.* **2002**, *8*, 876.
15. Tsukruk, V. V.; Genson, K.; Peleshanko, S.; Markutsya, S.; Lee, M.; Yoo, Y.-S. *Langmuir* **2003**, *19*, 495.
16. Samori, P.; Francke, V.; Mangel, T.; Müllen, K.; Rabe, J. P. *Opt. Mater.* **1998**, *9*, 390.
17. Xu, Z.; Holland, N. B.; Marchant, R. E. *Langmuir* **2001**, *17*, 377.
18. Jayaraman, M.; Frechet, J. M. J. *J. Am. Chem. Soc.* **1998**, *120*, 12996.
19. Ajayaghosh, A.; George, S. J. *J. Am. Chem. Soc.* **2001**, *123*, 5148.
20. Fu, H.-B.; Yao, J.-N. *J. Am. Chem. Soc.* **2001**, *123*, 1434.
21. Zheng, J.; Swager, T. M. *Macromolecules* **2006**, *39*, 6781.